Chapter 4

Is NADH a Donor for an Electron-Import PMOR?

4.1 Background

The majority of reported PMOR activities are electron export systems (Baker and Lawen, 2000; Kennett and Kuchel, 2003). Specifically, they transport electrons from *intracellular* electron donors to *extracellular* electron acceptors. In the previous Chapter I investigated the possibility that extracellular GSH could act as an electron donor for GSH bound to the inside of the cell membrane via a transmembrane thiol-disulfide exchange mechanism. Contrary to the report by Ciriolo and colleagues (1993), no such mechanism was identified. However, there are reports that another intracellular redox compound, NADH, when placed in the extracellular medium produces effects that are consistent with the concept of an electron import system (Zemkova, *et al.*, 1984; Birkmayer, *et al.*, 1993; Birkmayer, 1996; Forsyth, *et al.*, 1999; Slade, *et al.*, 1999; Nadlinger, *et al.*, 2002).

Extracellular NADH has been shown to have a hyperpolarising effect on mouse skeletal muscle plasma membranes (Zemkova, *et al.*, 1984). This hyperpolarising effect is inhibited by ouabain, an inhibitor of Na^+/K^+ ATPase, and PMOR inhibitors including adriamycin, pCMBS, and atebrin. In the process, NADH is oxidised and there is an apparent increase in K^+ membrane-permeability (Zemkova, *et al.*, 1984). Depolarisation of the membrane has been observed in the presence of extracellular AFR (Van Duijn, *et al.*, 2001b). These effects are similar to those observed with electron export NADH:(acceptor) oxidoreductases, and may imply that the action of extracellular NADH also involves a PMOR, and potentially an electron import system.

Nadlinger *et al.* (2002) have recently reported an *in vitro* assay using extracellular NADH as a measure of the intracellular ATP content of human RBCs. RBCs were withdrawn from healthy individuals immediately before and after exercise and incubated with 0.5 mM NADH. The rate of extracellular NADH oxidation by intact RBCs was faster in cells isolated after exercise than those isolated before, with 80-100% of the NADH oxidized after 2 h compared to 5% oxidized, respectively. After maximal aerobic activity the ATP-to-ADP ratio decreased to 80% of the baseline level, which correlated with the extent of NADH oxidation. The rate of NADH oxidation was dependent on the cell concentration (Nadlinger, *et al.*, 2002) suggesting that the RBCs were responsible for the effect. A mechanism linking extracellular NADH oxidation rates to intracellular ATP content was not established. However, if reducing equivalents from extracellular NADH could cross the membrane and reduce intracellular oxidised compounds, the rate of NADH oxidation would most likely reflect the oxidation state of the intracellular medium, which presumably would be more oxidised in ATP depleted cells.

Extracellular NADH also appears to have beneficial effects in the treatment of a number of diseases. NADH, given orally in a stabilised absorbable form, has been shown to have positive therapeutic effects on patients with Parkinson's disease (Birkmayer, *et al.*, 1993), Alzheimer's disease (Birkmayer, 1996) and chronic fatigue syndrome (Forsyth, *et al.*, 1999). The NADH is thought to alleviate motor and cognitive dysfunction by stimulating endogenous dopamine biosynthesis and by triggering energy production through ATP generation (Birkmayer, 1996). NADH has been shown to have a potent antiproliferative effect on the laryngeal carcinoma cell line Hep-2 and the murine fibrosarcoma cell line *in vitro*, but not on other carcinomas, possibly through DNA fragmentation and increased expression of p53 and Ki-67 (Slade, *et al.*, 1999).

It has also been suggested that extracellular NADH and NADPH have a protective effect against lipid peroxidation of human RBC membranes by cumene hydroperoxide (Yucel, *et al.*, 2000). These authors suggested that the protective effect of NAD(P)H was due to the release of peroxidases, such as GSHPx, into the supernatant by haemolysis; however there was no attempt to verify this claim.

4.2 Motivation

In this Chapter the possibility of transmembrane electron import across RBC plasma membranes using NADH was examined. NADH has a higher standard redox potential ($E^{\circ\prime}$= -320 mV) than GSH ($E^{\circ\prime}$= -230 mV) (Stryer, 1995), and thus might be expected to mediate electron import where GSH did not. The effect of NADH on RBC metabolism in glucose-deprived cells was monitored using ^{1}H and ^{31}P NMR. Various compounds were tested for their inhibitory effect on NADH-induced changes to RBC metabolism.

4.3 Results

4.3.1 ^{1}H NMR: effect of extracellular NADH on RBC metabolism

Incubation of human RBCs with extracellular NADH resulted in a change in the lactate-to-pyruvate ratio. In control, glucose-deprived, RBCs pyruvate accumulated over time more rapidly than lactate (Figure 4.1A), while if 5 mM NADH was added to the extracellular medium, a substantial amount of lactate was observed after 3 h with a corresponding small increase in pyruvate (Figure 4.1B). The resonance from NADH at 6.9 ppm was observed to decrease over the 3 h incubation with a concomitant increase in resonances from NAD^{+} between 8.5 and 9.5 ppm (Figure 4.1 inset).

Phase modulation of resonances in ^{1}H spin-echo NMR spectra due to spin-spin coupling made quantification difficult. The RBC lactate and pyruvate concentrations could however be estimated from the peak integral using calibration spectra. To make these, known concentrations of lactate and pyruvate were added to an RBC suspension and the integral relative to that of the reference compound (1 mM TSP) was measured.

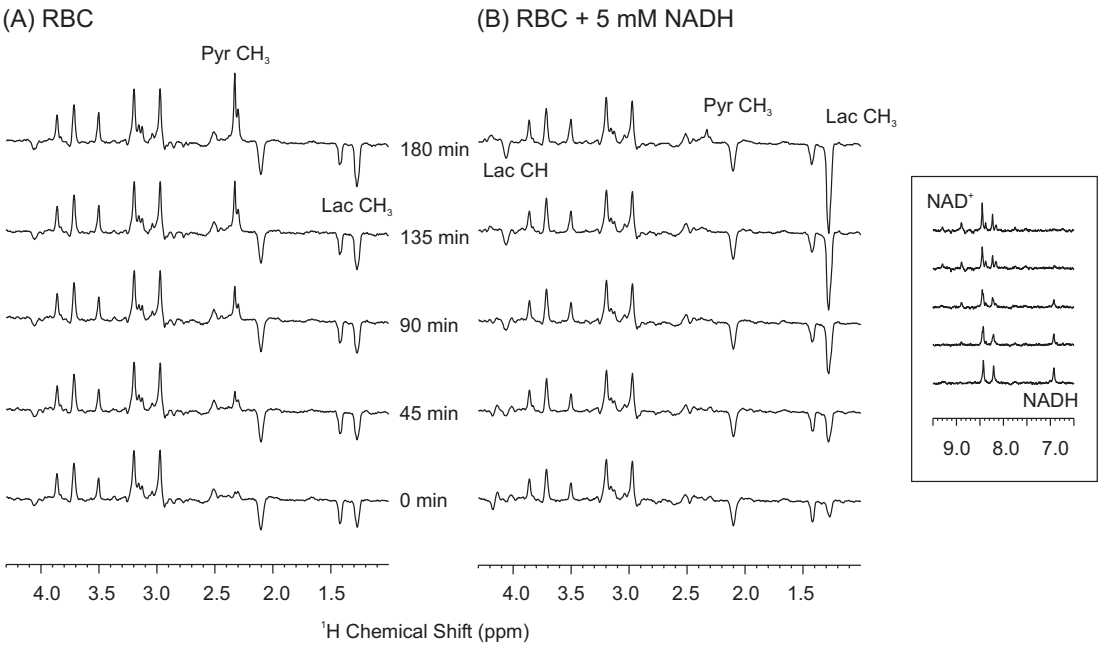

Figure 4.1: The change in ^{1}H spin-echo NMR spectra of glucose-deprived RBCs in 50 mM PBS, Hc = 0.65 over 3 h, (A) control and (B) with 5 mM NADH. Inset shows changes in NAD(H) peaks over the incubation period **(B)**. Peaks were calibrated to the external reference TSP $\delta(^{1}H)$ 0, and details of spectral acquisition are given in §2.5.4.

4.3.2 ^{1}H NMR: effect of PMOR inhibitors on NADH-induced changes to RBC metabolism

The rates of change in the lactate and pyruvate concentrations of glucose-deprived RBCs in the presence and absence of 5 mM NADH are shown in Figure 4.2. As discussed above there is a reversal in the lactate-to-pyruvate ratio on the addition of NADH to the suspension. The inhibitors atebrin (100 μM) and pCMBS (20 μM), which although not specific, have previously been shown to inhibit PMOR activity, had a small but statistically significant inhibitory effect on the rate of lactate production, but no effect on the rate of pyruvate formation (Figure 4.2). The sulfhydryl reagent NEM had no effect on the rates of formation of either lactate or pyruvate. The NADH oxidase inhibitor, capsaicin (100 μM) decreased the rate of lactate production in the presence of NADH, and increased the rate of pyruvate production with rates approaching those observed for glucose-deprived controls (Figure 4.2).

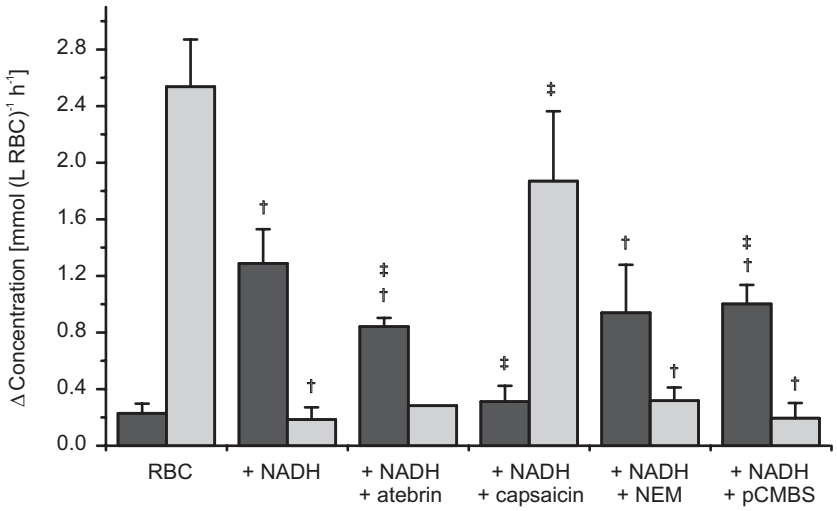

Figure 4.2: Rates of change of lactate (■) and pyruvate (■) concentrations in glucose-deprived RBCs incubated with 5 mM NADH and various PMOR inhibitors. RBCs in 50 mM PBS, Hc = 0.65, were incubated with no additions (n = 14); 5 mM NADH (n = 8); 5 mM NADH and 100 μM atebrin (n = 2); 5 mM NADH and 100 μM capsaicin (n = 3); 5 mM NADH and 20 μM NEM (n = 2); and 5 mM NADH and 20 μM pCMBS (n = 4). ^{1}H spin-echo NMR spectra were acquired at 10 min intervals over 1.5 h at 37 °C and the lactate and pyruvate concentrations were estimated from the lactate-CH_3 and pyruvate-CH_3 peak integrals, respectively. The rate of change in concentration was calculated over the whole of the 1.5 h incubation. Error bars denote ± 1 s.d. Data were analysed for a statistically significant difference from controls ($p < 0.05$) using the non-parametric Mann-Whitney U test; † denotes rates with $p < 0.05$ when compared to RBCs with no additions; ‡ denotes rates with $p < 0.05$ when compared to RBCs incubated with 5 mM NADH.

4.3.3 ^{1}H NMR: effect of membrane transport inhibitors on NADH-induced changes to RBC metabolism

The effects of the band-3 anion exchange inhibitor 4,4′-diisothiocyanatostilbene-2,2′-disulfonic acid (DIDS; Figure 4.3) and the monocarboxylate transport inhibitor α-cyano-4-hydroxycinnamate (αCHC; Figure 4.3) on the NADH-induced changes in RBC metabolism were investigated. Incubation of RBCs with 0.1 mM DIDS for 1 h prior to addition of NADH had no effect on the NADH-induced changes to RBC metabolism (Figure 4.4). In contrast, incubation of RBCs with 50 mM αCHC, in the absence of NADH, increased the rate of lactate production and decreased the rate of pyruvate production (Figure 4.4). In the presence of NADH the rate of lactate production was slightly attenuated when compared to cells not exposed to αCHC (Figure 4.4).

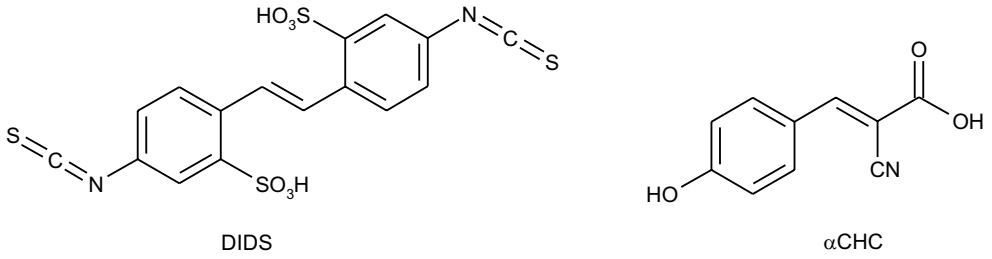

DIDS αCHC

Figure 4.3: The band 3 anion-exchange inhibitor DIDS and the monocarboxylate transport inhibitor αCHC

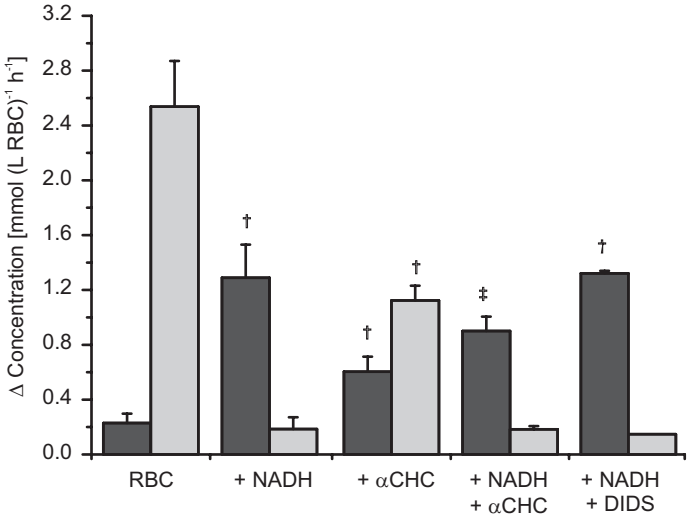

Figure 4.4: Rates of change of lactate (■) and pyruvate (■) concentrations in glucose-deprived RBCs incubated with 5 mM NADH and inhibitors of band 3 and the monocarboxylate transporter. ^{1}H spin-echo NMR spectra of RBCs in 50 mM PBS, Hc = 0.65, with no additions (n = 14); 5 mM NADH (n = 8); 50 mM αCHC (n = 5); 5 mM NADH and 50 mM αCHC (n = 4); and 5 mM NADH and 0.1 mM DIDS (n = 2) were acquired at 10 min intervals over 1.5 h at 37 °C. RBCs were incubated for 1 h at 37 °C with αCHC or DIDS then washed prior to acquisition (and addition of NADH). The lactate and pyruvate concentrations were estimated from the lactate-CH_3 and pyruvate-CH_3 peak integrals, respectively. The rate of change in concentration was calculated over the whole of the 1.5 h incubation. Error bars denote ± 1 s.d. Data were analysed for a statistically significant difference from controls ($p < 0.05$) using the non-parametric Mann-Whitney U test; † denotes rates with $p < 0.05$ when compared to RBCs with no additions; ‡ denotes rates with $p < 0.05$ when compared to RBCs incubated with 5 mM NADH.

4.3.4 ^{31}P NMR: effect of NADH and membrane transport inhibitors on RBC metabolism

The effects of DIDS and αCHC on the concentrations of the main phosphorus-containing compounds in RBCs were investigated by ^{31}P NMR and compared to those observed in the presence of NADH. The dominant resonances in a ^{31}P NMR spectrum of glucose-deprived RBCs (in PBS) are from the two phosphorus atoms of 2,3BPG, and from intra- and extracellular orthophosphate (P_i); the concentration of ATP in glucose-deprived cells was too low for the three ATP-phosphate peaks to be observed above the noise (Figure 4.5).

Some phosphorus compounds, such as P_i, have different chemical shifts depending on whether they are in the intra- or extracellular environment (Kirk and Kuchel, 1988b). The difference in chemical shift is caused by a difference in magnetic susceptibility in the two compartments as well as direct effects of proteins in the intracellular space. The presence of oxy- or carbon monoxyHb makes the cytoplasm more diamagnetic than the extracellular medium, lowering the magnetic field strength in the internal compartment (Kirk and Kuchel, 1988b). The presence of Hb in the intracellular space also changes the hydrogen bonding experienced by the phosphorus molecules, decreasing the chemical shift of the intracellular molecule (Kirk and Kuchel, 1988a).

The chemical shifts and change in peak integrals of ^{31}P NMR spectra over time give an indication of the change in pH (see §4.3.5) of the suspension and the utilisation of the key energy supplying molecules. In glucose-deprived RBCs the main metabolite is 2,3BPG, which is involved in regulation of oxygen dissociation from Hb, and normally exists at a concentration of 4.17 ± 0.64 mmol (L RBC)$^{-1}$ (Beutler, 1984). 2,3BPG is metabolised through the reactions in the lower part of the glycolytic pathway, and in the absence of NAD^+ recycling at GAPDH, pyruvate and NAD^+ accumulate and ADP is phosphorylated at the pyruvate kinase reaction.

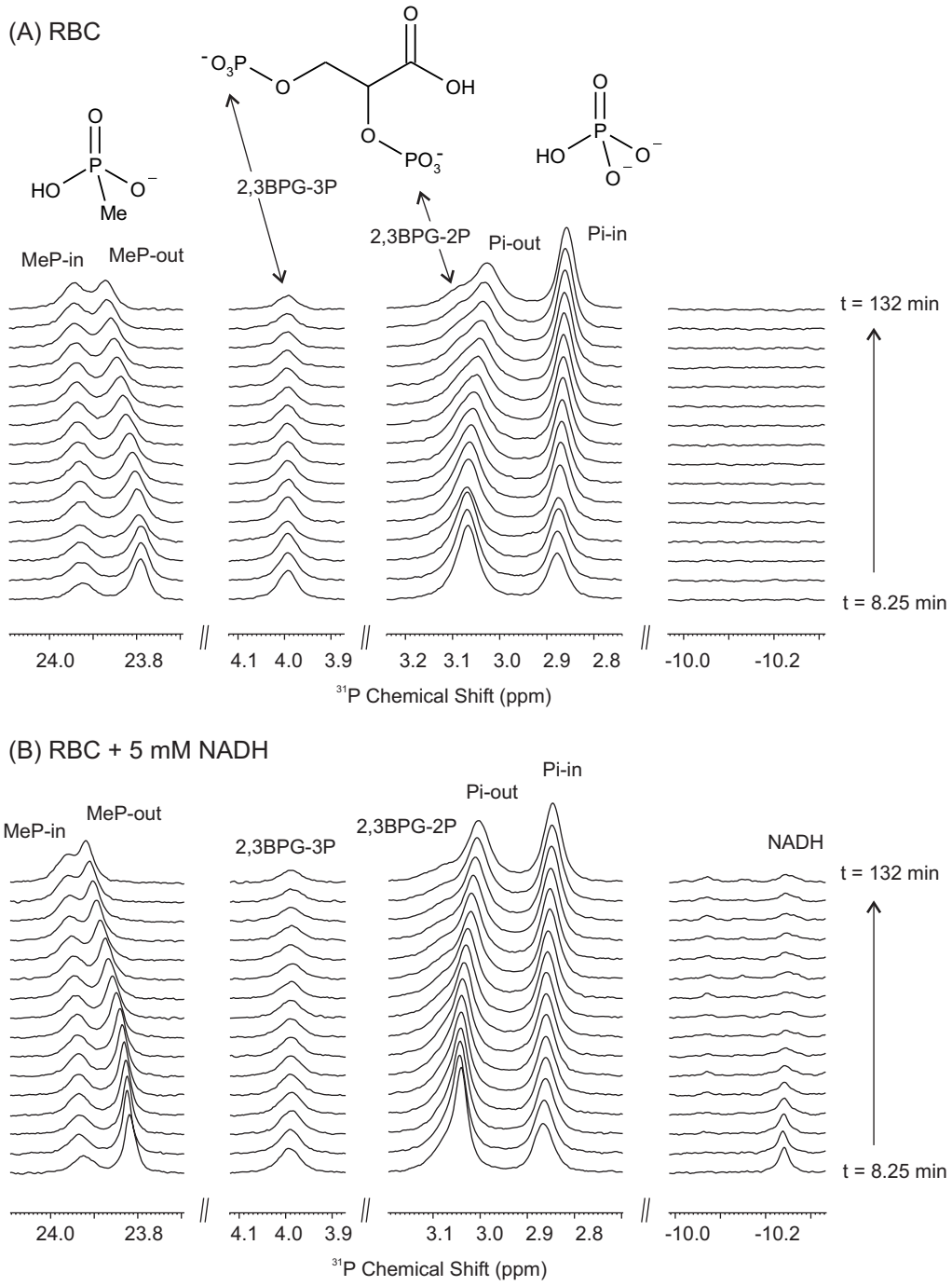

Figure 4.5: ^{31}P NMR spectra of (A) glucose-deprived RBCs and (B) the same cells incubated with 5 mM NADH, over 2 h timecourse. RBCs in 25 mM PBS, Hc = 0.68, containing 9.7 mM TEP were incubated for 30 min at 37 °C with 5 mM MeP prior to spectral acquisition to provide a pH reference. ^{31}P NMR spectra were acquired at 8.25 min intervals over 132 min. Chemical structures of phosphorus compounds giving rise to the major peaks are shown for reference. The abbreviations used are MeP, methylphosphonate; 2,3BPG, 2,3-*bis*phosphoglycerate; P_i, orthophosphate. Spectra were referenced to TEP $\delta(^{31}P)$ 0.44. Details of spectral acquisition are given in §2.5.4.

In control glucose-deprived RBCs the concentration of 2,3BPG decreased over 2 h, while the concentration of P_i slowly increased (Figures 4.5 and 4.6). Changes in the chemical shift of the intra- and extracellular P_i peaks suggested that the pH changed during the timecourse (see §4.3.5). Inclusion of NADH in the incubation did not appear to affect the rate of 2,3BPG decline or the rate of P_i equilibration across the membrane (Figures 4.5 and 4.6).

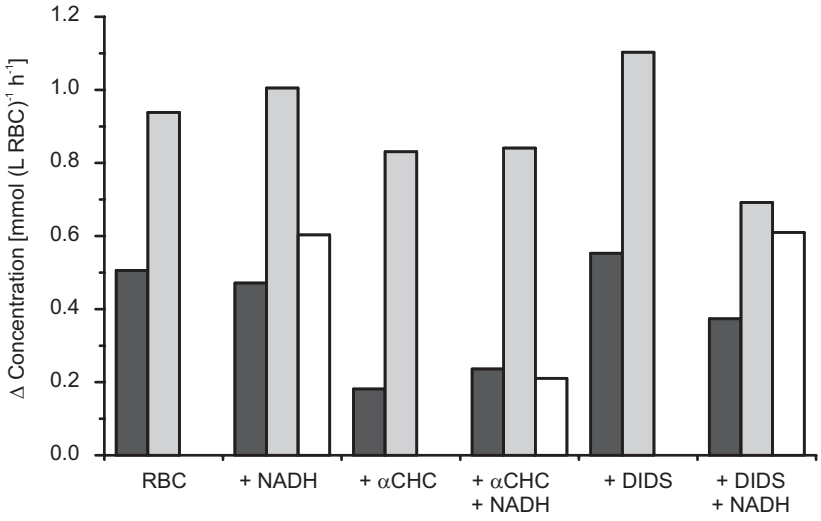

Figure 4.6: Rate of decrease of 2,3BPG (■), increase of intracellular P_i (▒) and decrease of NADH (□) concentrations in glucose-deprived RBCs incubated with NADH and various membrane transport inhibitors. RBCs in 25 mM PBS, Hc = 0.68; with 5 mM NADH; 50 mM αCHC; 5 mM NADH and 50 mM αCHC; 0.1 mM DIDS; and 5 mM NADH and 0.1 mM DIDS. RBCs were incubated for 1 h at 37 °C with DIDS or αCHC then washed prior to spectral acquisition (and addition of NADH). ^{31}P NMR spectra were acquired at 8.25 min intervals over 132 min at 37 °C. The concentrations of 2,3BPG, intracellular P_i, and NADH were determined from their respective integrals in ^{31}P spectra (the 2,3BPG concentration was determined from the 3P peak, as the 2P peak was obscured by extracellular P_i). The rate was taken over the whole 132 min incubation for 2,3 BPG and intracellular P_i, and until the peak disappeared into the noise for NADH.

Incubation of RBCs with 50 mM αCHC more than halved the rate of 2,3BPG utilisation in both the presence and absence of NADH. The rate of entry of P_i into the cells was also slightly lower in these cells than in controls (Figure 4.6). The rate of NADH oxidation by RBCs exposed to αCHC was also significantly lower than in control RBCs incubated with extracellular NADH (Figure 4.6).

The band-3 anion-exchange inhibitor DIDS was expected to inhibit the entry of P_i into the RBCs; however incubation with 0.1 mM DIDS increased the rate of intracellular P_i accumulation and marginally increased the rate of 2,3BPG decline (Figure 4.6). The addition of NADH markedly decreased the rate of uptake of P_i, slightly decreased the rate of 2,3BPG decline, and had no effect on the NADH oxidation rate compared to control cells exposed to NADH (Figure 4.6).

4.3.5 ^{31}P NMR: effect of membrane transport inhibitors on RBC pH

The intra- and extracellular pH in a RBC suspension can be calculated from the chemical shift differences between MeP and P_i. Both MeP and P_i experience different intra- and extracellular environments and thus give rise to separate peaks in ^{31}P NMR spectra. The chemical shifts of MeP and P_i are also pH sensitive; the peaks from MeP move to higher chemical shift with a decrease in pH, and those from P_i move to a lower chemical shift (Stewart, *et al.*, 1986). Stewart *et al.* (1986) showed that the observed chemical shift (δ) of a pH sensitive compound depends on the concentration of the acid and base forms of the compound [A^-] and [HA], and the chemical shifts of the acid ($^a\delta$) and base ($^b\delta$) forms, respectively:

$$\delta = \frac{[A^-]^b\delta + [HA]^a\delta}{[HA] + [A^-]}$$

Thus the Henderson-Hasselbalch equation becomes:

$$pH = pKa' + \log_{10}\left(\frac{\delta - {}^a\delta}{{}^b\delta - \delta}\right)$$

where pKa′ is the apparent pKa. In the case of MeP the values of pKa′, $^a\delta$ and $^b\delta$ in plasma or plasma-like solutions are 7.52 ± 0.01, 25.208 ± 0.003 and 21.259 ± 0.035, respectively (Stewart, *et al.*, 1986). Thus from the observed intra- and extracellular chemical shifts for MeP the pH of the intra- and extracellular compartments can be determined.

In control RBCs and those incubated with 5 mM NADH the intracellular pH was initially 7.2 and decreased by ~0.01 pH over the 2 h incubation; the pH decreased slightly faster in the presence of NADH (Figure 4.7A). The extracellular pH (~7.27) was initially higher than the intracellular pH (~7.2) for both the RBC control and

cells exposed to NADH. After an initial lag, the extracellular pH decreased in both cases by ~0.04 pH units over the 2 h incubation (Figure 4.7B).

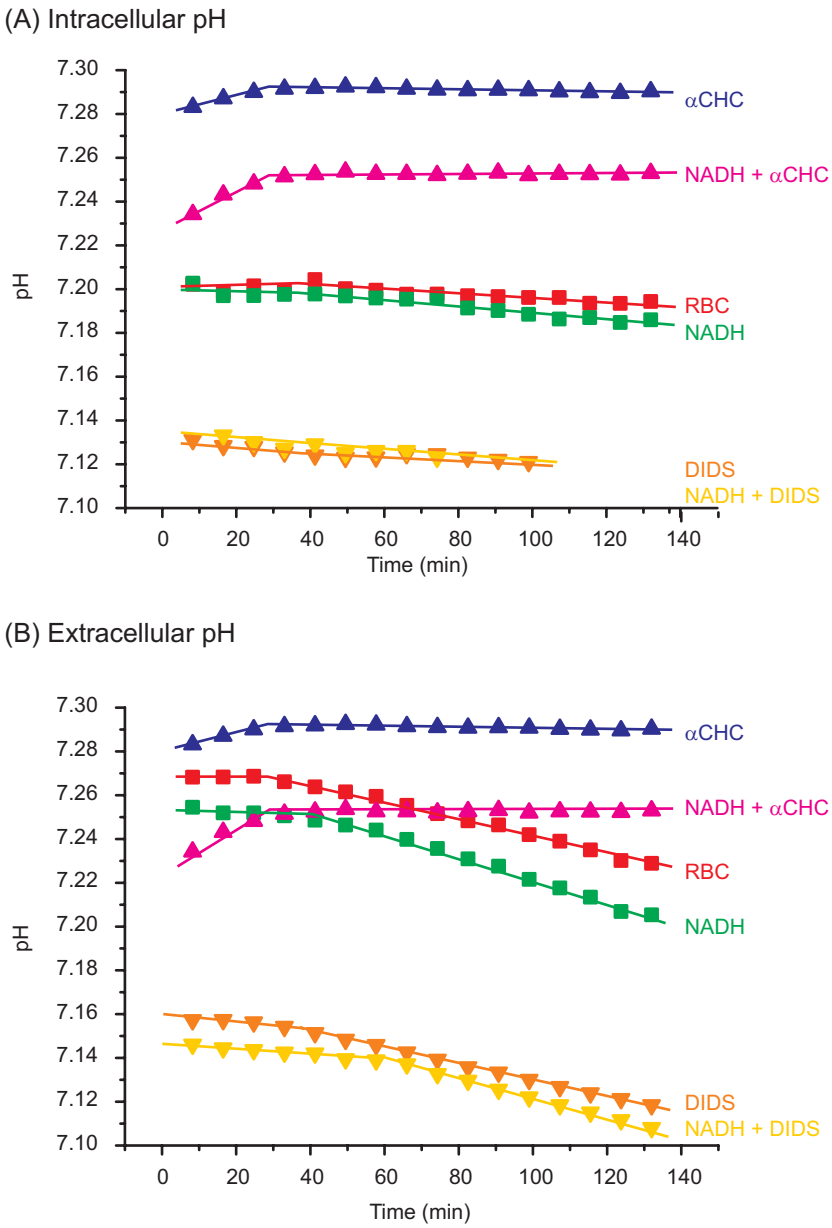

Figure 4.7: Change in intracellular (A) and extracellular (B) pH in glucose-deprived RBCs incubated with NADH and various membrane transport inhibitors. RBCs in 25 mM PBS, Hc = 0.68, containing 9.7 mM TEP were incubated with 5 mM MeP for 30 min at 37 °C prior to acquisition of ^{31}P NMR spectra. RBCs were incubated with no additions (■); 5 mM NADH (■); 50 mM αCHC (▲); 50 mM αCHC and 5 mM NADH (▲); 0.1 mM DIDS (▼); and 0.1 mM DIDS and 5 mM NADH (▼). RBCs were washed after incubation for 1 h at 37 °C with αCHC and DIDS prior to addition of MeP and acquisition of spectra. The intra- and extracellular pH were determined using the method of Stewart *et al*. (1986) as described in the text.

In RBCs incubated with αCHC prior to the addition of NADH, the intra- and extracellular MeP peaks were overlapped. Thus, without suppressing the signal from extracellular MeP, i.e., with manganese chloride (Stewart, *et al.*, 1986), it was not possible to determine the intra- and extracellular pH separately. The approximate pH of the whole solution was determined from the observed chemical shift of MeP; it initially increased by 0.01 pH units in the absence of NADH and increased by 0.02 pH units in the presence of NADH. The pH did not appear to change for the remainder of the timecourse. The starting pH in the presence of NADH (pH 7.23) was lower than in its absence (pH 7.28; Figure 4.7).

DIDS inhibits the uptake of MeP by RBCs (Stewart, *et al.*, 1986). The observation of intra- and extracellular MeP peaks in RBCs incubated with 0.1 mM DIDS for 1 h prior to the addition of MeP, suggests that incomplete inhibition of band 3 occurred. The intra- and extracellular pH values for cells incubated with DIDS were lower than those observed for control cells, pH ~7.13 and ~7.16 in the absence and presence of NADH, respectively. However the rate of change of pH over the 2 h incubation was similar to that observed in controls (Figure 4.7). After approximately 80 min of incubation the intra- and extracellular MeP peaks were superimposed.

4.3.6 ^{1}H NMR: effect of glucose on NADH-induced changes in RBC metabolism

The rates of lactate and pyruvate formation by glucose-deprived RBCs incubated with 5 mM NADH were compared to their rate of formation in the presence of 10 mM glucose. The rate of lactate formation was significantly faster in glucose-supplied RBCs compared to those deprived of glucose in both the presence and absence of NADH (Figure 4.8). The addition of NADH to glucose supplied RBCs had no affect on the rates of lactate or pyruvate production over glucose-supplied control RBCs (Figure 4.8).

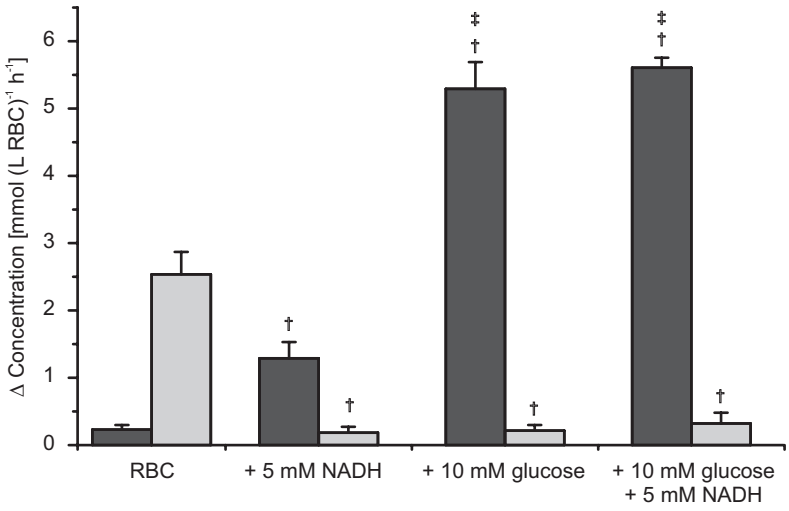

Figure 4.8: Effect of glucose on the rates of change of lactate (■) and pyruvate (■) concentrations in RBCs incubated with and without 5 mM NADH. ^{1}H spin-echo NMR spectra of RBCs in 50 mM PBS, Hc = 0.65, with the indicated additions, were acquired at 10 min intervals over 1.5 h at 37 °C. The lactate and pyruvate concentrations were estimated from the lactate-CH_3 and pyruvate-CH_3 peak integrals, respectively, and the rate of change over the 1.5 h incubation calculated. Data represent the average of three separate experiments and error bars denote ± 1 s.d. Data were analysed for a statistically significant difference from controls ($p < 0.05$) using the non-parametric Mann-Whitney U test; † denotes rates with $p < 0.05$ when compared to RBCs with no additions; and ‡ denotes rates with $p < 0.05$ when compared to RBCs incubated with 5 mM NADH.

4.3.7 ^{1}H NMR: effect of NADD on the end products of RBC metabolism

In an attempt to clarify the location of the effect of NADH, intra- or extracellular, RBCs were incubated with NADD. If NADD and LDH are in the same compartment then lactate deuterated at the C-2 position [2-^{2}H]lactate can be formed (Figure 4.9). In ^{1}H spin-echo NMR spectra of RBCs with τ = 68 ms, the CH_3 peak of fully protonated lactate, [2-^{1}H]lactate, is inverted due to spin-spin coupling between the CH and CH_3 protons (Brown, *et al.*, 1977; Berthon and Kuchel, 1995). In [2-^{2}H]lactate the phase modulation due to homonuclear coupling is removed and the methyl resonance is upright (positive phase). Spectra of mixed [2-^{1}H]- and [2-^{2}H]lactate, provided appropriate line broadening functions are applied, appear to have a symmetrical phase inversion about the baseline (Berthon and Kuchel, 1995).

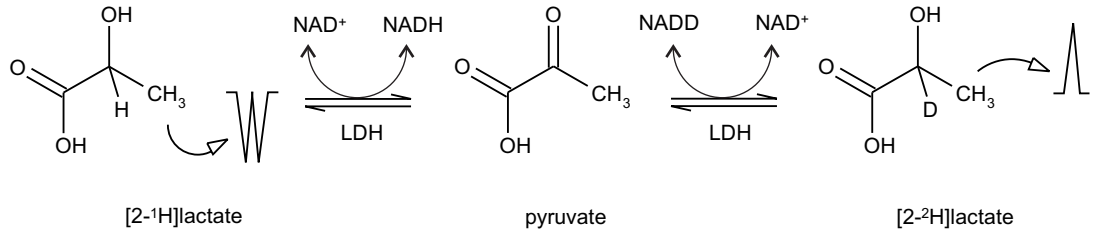

Figure 4.9: Isotope exchange at the LDH reaction and its effect on the ^{1}H NMR spin-echo spectrum of the lactate methyl resonance.

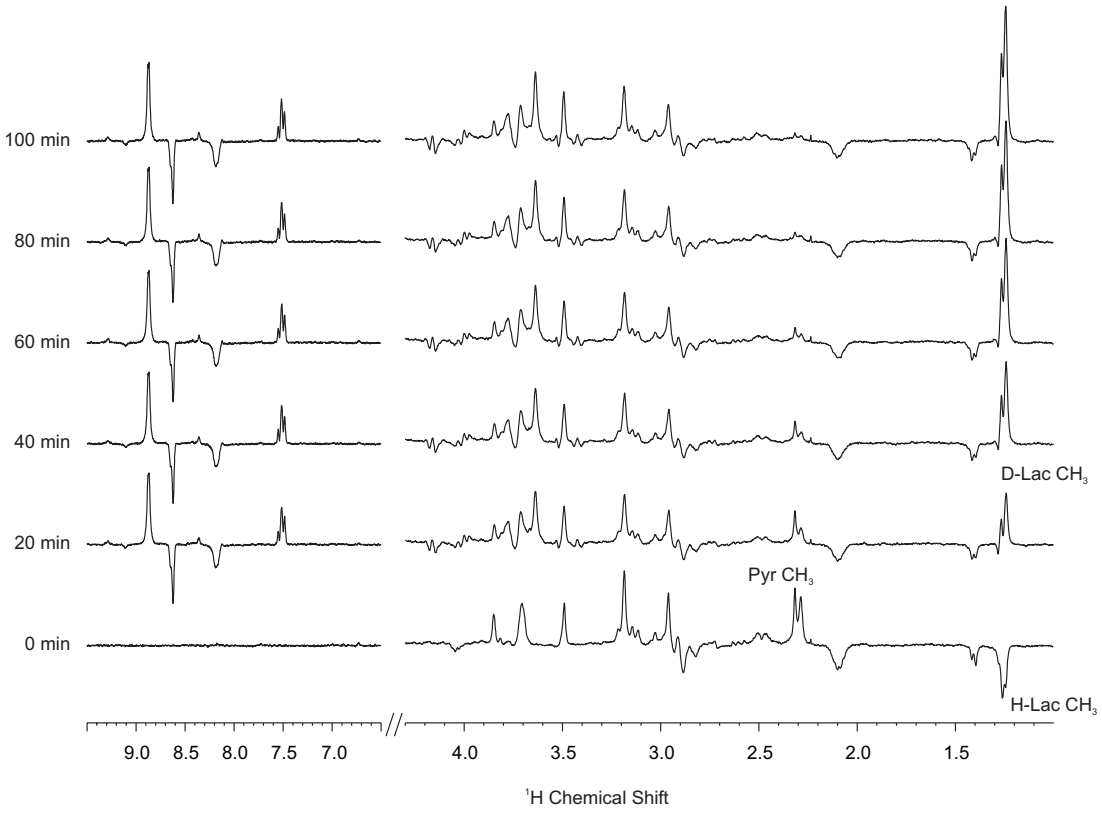

Figure 4.10: Effect of NADD on the ^{1}H spin-echo NMR spectra of glucose-starved RBCs. RBCs in 50 mM PBS, Hc = 0.65, were incubated with 5 mM NADD at 37 °C and ^{1}H spin-echo NMR spectra acquired at 10 min intervals over 2 h. Peaks were calibrated to the external reference TSP $\delta(^{1}H)$ 0. Details of spectral acquisition are given in §2.5.4. Abbreviations: D-Lac CH_3, [2-^{2}H]lactate-CH_3; H-Lac CH_3, [2-^{1}H]lactate-CH_3; Pyr CH_3, pyruvate-CH_3.

Incubation of RBCs starved of glucose for 2 h with NADD resulted in the appearance of an upright peak immediately to lower frequency of the inverted endogenous lactate peak (Figure 4.10). This peak increased markedly over the 2 h incubation, and the majority of lactate at the end of the incubation was [2-^{2}H]lactate. The intensity of the pyruvate-CH_3 resonance decreased over the incubation time. There was no apparent effect on resonances from other metabolites and compounds

in the RBC suspension. The inclusion of 30 mM nicotinamide in the suspension medium, to inhibit the activity of NADases (Kuchel and Chapman, 1985), obscured the signals from NADD (Figure 4.10), hence the rate of NADD oxidation could not be established from these experiments.

4.3.8 ^{1}H NMR: effect of pyruvate on NADH-induced changes in RBC metabolism

The formation of [2-^{2}H]lactate in the experiments described in §4.3.7 could be due to the presence of LDH in the extracellular compartment. To investigate this effect further, RBCs were incubated with 5 mM NADH in the presence of 5 mM pyruvate. In contrast to RBCs incubated with NADH in the absence of pyruvate (Figure 4.1), inclusion of pyruvate in the incubation medium led to a biphasic pattern of lactate formation (Figure 4.11A). The lactate concentration initially increased rapidly, with a concomitant decrease in the pyruvate concentration. After approximately 12 min the rates of change of lactate and pyruvate decreased to much lower values than observed in the first half of the timecourse (Figure 4.11A).

The PMOR inhibitors, 100 μM atebrin, 20 μM NEM and 20 μM pCMBS, had no effect on the initial rate of lactate formation in RBCs supplied with 5 mM pyruvate and 5 mM NADH (Figure 4.11B). The NADH oxidase inhibitor capsaicin (100 μM) changed the initial rate of lactate formation; in these experiments capsaicin stimulated the production of lactate and pyruvate (Figure 4.11B).

The final rate of lactate formation in the presence of atebrin and pCMBS was similar to that observed in the control experiment. A markedly slower rate of lactate production was observed in the presence of capsaicin and NEM. The final rate of pyruvate production was lower in the presence of all the inhibitors than that observed in controls (Figure 4.11C).

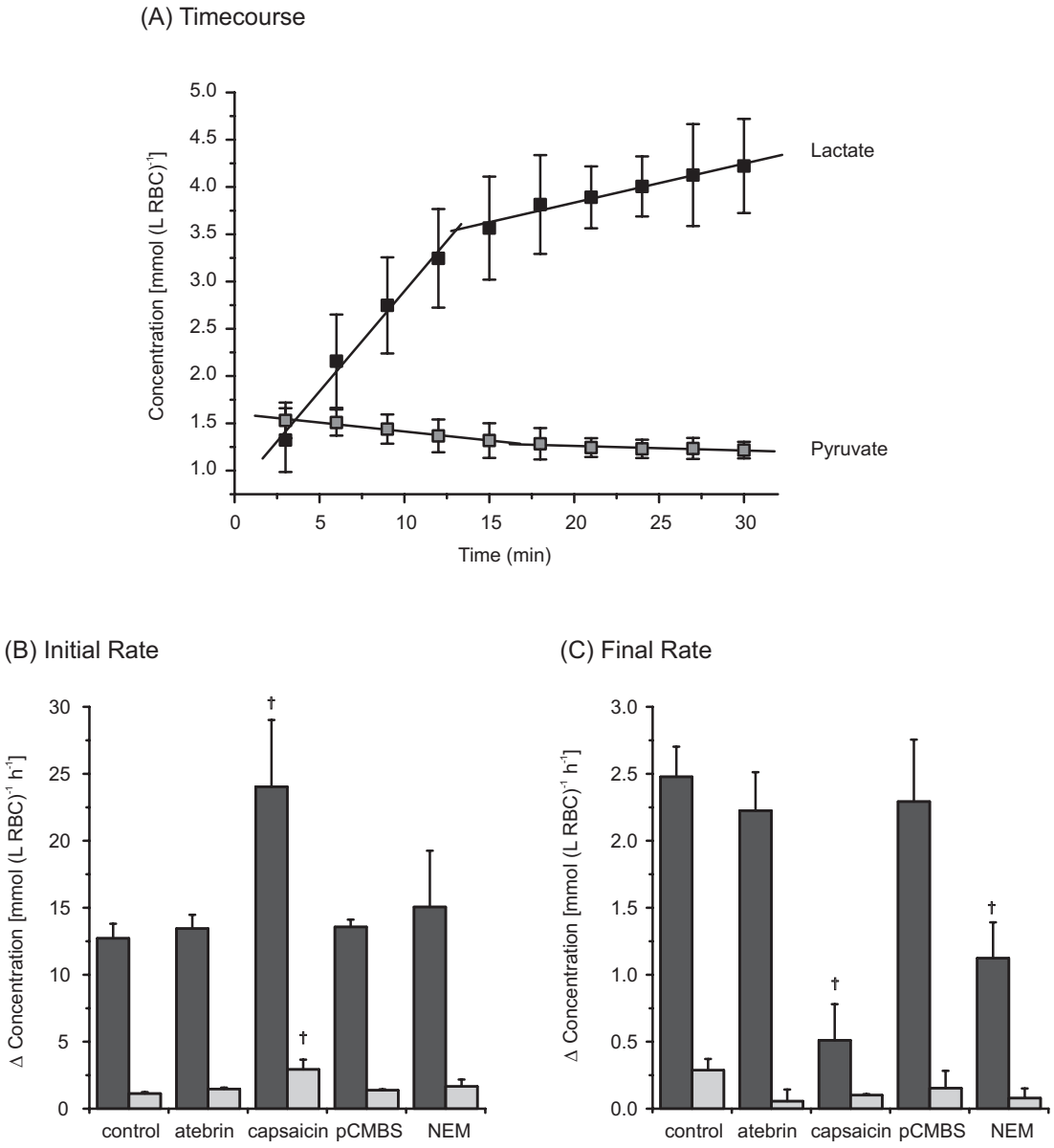

Figure 4.11: Changes in lactate (■) and pyruvate (■) concentrations in glucose-deprived RBCs incubated with 5 mM pyruvate and 5 mM NADH in the presence and absence of various inhibitors of PMORs. ^{1}H spin-echo NMR spectra of RBC in 2 mM PBS, Hc = 0.65, incubated with 5 mM pyruvate and 5 mM NADH (control) in the presence of: 100 μM atebrin; 100 μM capsaicin; 20 μM pCMBS; 20 μM NEM. The spectra were acquired at 3 min intervals over 30 min at 37 °C. **(A)** The change in the lactate and pyruvate concentration in control incubations, **(B)** the initial, and **(C)** the final rates of lactate and pyruvate formation. The lactate and pyruvate concentrations were estimated from the lactate-CH_3 and pyruvate-CH_3 peak integrals, respectively . Data represent the average of six separate experiments, and error bars denote ± 1 s.d. Data were analysed by the non-parametric Mann-Whitney U test for statistically significant differences from controls ($p < 0.05$); and † denotes rates that had $p < 0.05$ compared to RBCs incubated with 5 mM NADH and 5 mM pyruvate.

4.3.9 Spectrophotometric assays: effect of pyruvate on the rate of NADH oxidation

Because of the rapid rate of NADH oxidation by RBCs incubated with NADH and pyruvate and the low signal to noise of the NADH resonance in ^{1}H spin-echo NMR spectra, it was difficult to determine the rate of NADH oxidation accurately. The rate of NADH oxidation was more readily established by spectrophotometric methods (Figure 4.12). In the absence of pyruvate the rate of NADH oxidation by glucose-deprived RBCs was slow (0.84 mM^{-1} h^{-1}) while in the presence of 5 mM pyruvate it was rapid (9.06 mM^{-1} h^{-1}). The NADH was nearly completely oxidised after 30 min.

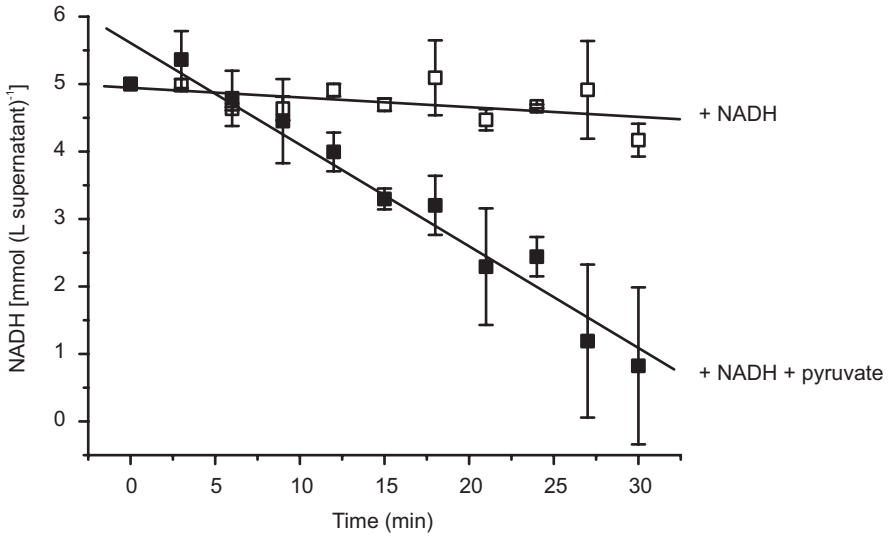

Figure 4.12: Spectrophotometric assay of NADH oxidation in the supernatant of RBCs. RBCs in 2 mM PBS, Hc = 0.65, were incubated with 5 mM NADH (□), or 5 mM NADH and 5 mM pyruvate (■) for 30 min at 37 °C. The supernatant was separated from the cells by centrifugation through dibutyl phthalate and the NADH concentration calculated from the optical density at 340 nm and the extinction coefficient for NADH (ε_{340} = 6.22 $mM^{-1}cm^{-1}$). Data represent the average of two separate experiments and error bars denote ± 1 s.d. Lines of best fit are shown. The rate of NADH oxidation in the absence of pyruvate was 0.84 mmol (L supernatant)$^{-1}$ h^{-1}, and in the presence of 5 mM pyruvate, 9.06 mmol (L supernatant)$^{-1}$ h^{-1}.

4.3.10 ^{1}H NMR: effect of LDH inhibitors on NADH-induced changes in RBC metabolism

The rapid conversion of pyruvate to lactate by glucose-deprived RBCs incubated with NADH and pyruvate again suggested a role for LDH in the observed changes in the end products of RBC metabolism. LDH activity can be inhibited by oxalate and oxamate (Simpson, *et al.*, 1982; Mazo, *et al.*, 1990). These compounds had a concentration-dependent inhibitory effect on the rates of lactate production, pyruvate utilisation, and NADH oxidation by RBCs exposed to NADH and pyruvate (Figure 4.13). Oxalate at 10 mM inhibited the rate of lactate formation by 80% (Figure 4.13A), while 10 mM oxamate inhibited the rate of lactate formation by 60% (Figure 4.13B).

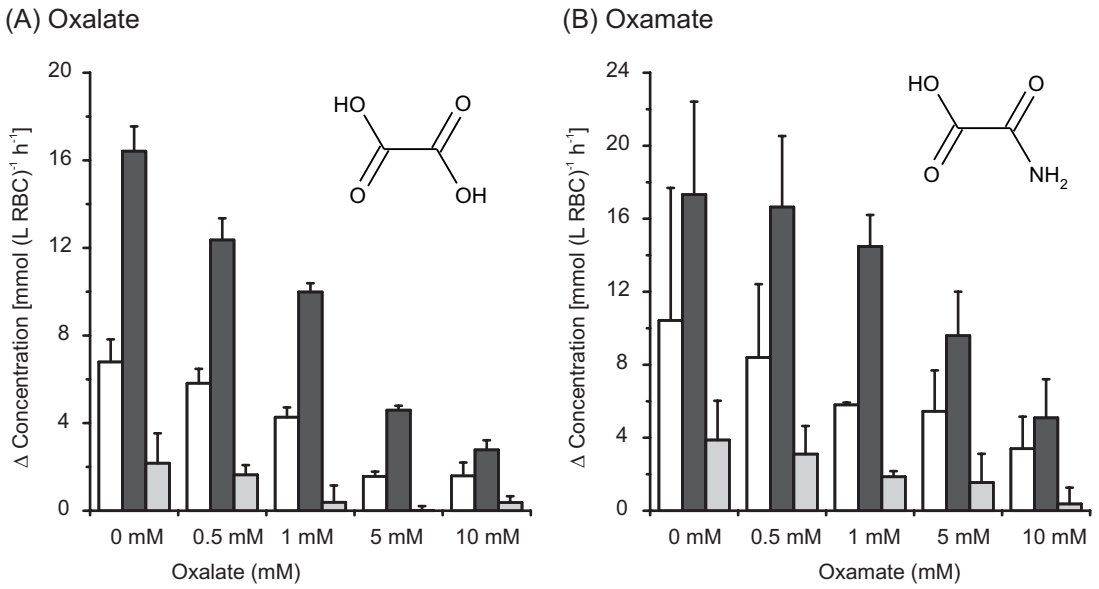

Figure 4.13: Effect of the LDH inhibitors oxalate (A) and oxamate (B) on the rates of NADH oxidation (□), lactate formation (■), and pyruvate utilisation (■). ^{1}H spin-echo NMR spectra of RBCs in 2 mM PBS, Hc = 0.65, incubated with 5 mM pyruvate and 5 mM NADH in the presence of increasing concentrations of **(A)** oxalate and **(B)** oxamate were acquired at 3 min intervals over 30 min at 37 °C. The lactate, pyruvate, and NADH concentrations were estimated from the lactate-CH_3, pyruvate-CH_3, and NADH δ(^{1}H) 6.99 peak integrals, respectively and the initial rate calculated. Data represent the average of two separate experiments and error bars denote ± 1 s.d. The chemical structures of oxalate and oxamate are shown for reference.

Pre-incubation of RBCs with oxalate or oxamate allowed equilibration of these molecules across the plasma membrane, and increased the inhibition of intracellular

LDH. The initial rate of lactate formation by glucose-deprived RBCs in the presence of NADH and pyruvate was inhibited 75% by 5 mM oxalate and 44% by 5 mM oxamate (Table 4.1). Pre-incubation with oxalate or oxamate decreased the control rate of lactate production by 16 and 32%, respectively, and the addition of oxalate or oxamate to the cells already exposed to these inhibitors decreased the rate of lactate production to a greater extent than observed without pre-incubation (Table 4.1).

Table 4.1: Effect of inhibiting LDH with oxalate or oxamate on the initial rates of lactate production in glucose-deprived human RBCs incubated with 5 mM pyruvate and 5 mM NADH. RBCs were incubated at 37 °C for 1 h in 2 mM PBS with no additions (control), 5 mM oxalate, and 5 mM oxamate. RBCs were washed twice with 2 mM PBS prior to addition of pyruvate, NADH, and the inhibitors, and acquisition of ^{1}H spin-echo NMR spectra.

Pre-incubation condition	Control	+ 5 mM oxalate	+ 5 mM oxamate
	% inhibition of initial rate of lactate production		
PBS	0	75 ± 2	44 ± 10
+ 5 mM oxalate	16 ± 1	81 ± 1	-
+ 5 mM oxamate	32 ± 3	-	50 ± 10

4.3.11 Spectrophotometric assays: extent of haemolysis

To establish the extent of haemolysis during the starvation incubation period the LDH activity released into the supernatant was compared to the LDH activity of intact cells. Haemolysis, based on the percentage of LDH leaked from RBCs, increased over the incubation time at 37 °C, with a rate of increase of 1.16% h^{-1}. The maximum amount of haemolysis observed was 5% at 3 h.

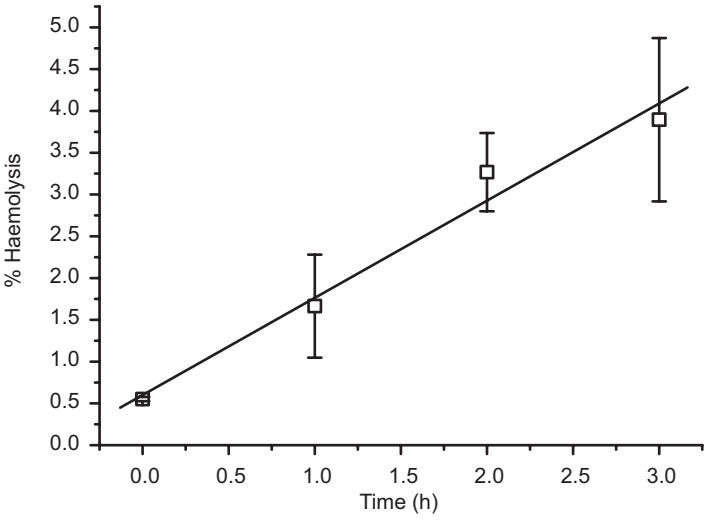

Figure 4.14: Extent of haemolysis. RBCs were incubated in 50 mM PBS, Hc = 0.65, for 3 h at 37 °C. The % haemolysis was determined from the activity of LDH (see §2.4.3) in the supernatant and whole cells. The data points represent the average of two separate experiments and error bars denote ± 1 s.d. The line of best fit is shown: % haemolysis = 0.60 + 1.16 × time (h).

4.4 Discussion

NADH in the extracellular medium is oxidised by glucose-deprived RBCs. The oxidation of NADH is concomitant with an increase in the rate of lactate production above that seen in control glucose-deprived RBCs (Figures 4.1 and 4.2). The rate of lactate formation in the presence of NADH was significantly lower than that obtained from glucose supplied cells (Figure 4.8). Additionally, exposure to NADH of cells supplied with glucose did not appear to have an increased rate of lactate production above that observed in its absence (Figure 4.8). Thus the oxidation of NADH and its effect on RBC metabolism appears to be specific to cells under starvation-induced stress.

In the absence of glucose, NADH recycling at GAPDH is no longer possible, hence pyruvate formed from the metabolism of 2,3BPG can not be converted to lactate, the usual end product of human RBC glycolysis. The increased rate of lactate formation by glucose-starved cells in the presence of extracellular NADH may indicate an increase in the intracellular NADH-to-NAD^+ ratio, through transmembrane exchange of reducing equivalents.

The rate of lactate formation by glucose-deprived RBCs was slightly lower in the presence of the PMOR inhibitors atebrin and pCMBS. The sulfhydryl reagent NEM had no effect on the rate of lactate or pyruvate formation (Figure 4.2). The NADH oxidase inhibitor capsaicin substantially inhibited the rate of lactate production and stimulated the rate of pyruvate formation. The rates observed with capsaicin were not found to be significantly different from those observed in control glucose-starved cells. This strong inhibition suggested the possible involvement of a plasma membrane NADH oxidase activity.

Glucose-deprived RBCs exposed to 5 mM pyruvate and 5 mM NADH also exhibited a change in the lactate-to-pyruvate ratio (Figure 4.11). Under these conditions the formation of lactate was biphasic, with an initial rapid increase in lactate, concomitant with a decrease in NADH and pyruvate concentrations. After 15 min the rate of lactate formation decreased and the rate of pyruvate utilization slowed (Figure 4.11A). The rate of NADH oxidation was significantly faster in the presence of excess extracellular pyruvate than in its absence (Figure 4.12), but did not show the same biphasic trend as observed for the changes in lactate and pyruvate concentration, suggesting that the effect on these compounds is dependent on the concentration of NADH. The PMOR inhibitors atebrin, NEM and pCMBS had no effect on the initial rate of lactate formation, while capsaicin, in contrast to the inhibition observed in the absence of pyruvate, stimulated the initial rate of lactate formation (Figure 4.11B). The vanilloid capsaicin is a ubiquinone analogue (Vaillant, *et al.*, 1996), so changes in activity by capsaicin may reflect the involvement of CoQ in the process. The initial rates of lactate production and pyruvate utilisation were also significantly faster in the presence of added pyruvate than in its absence, but the final rates of formation were similar to those observed over the whole incubation in the absence of pyruvate.

It was initially postulated that these results reflected the activity of a transmembrane NADH oxidase, allowing the transfer of reducing equivalents from extracellular NADH to intracellular NAD^+ and thus forming intracellular lactate. In order to verify this hypothesis the effect of NADH oxidation on the intra- and extracellular

pH was investigated by ^{31}P NMR. It was found that in both the presence and absence of extracellular NADH, the intra- and extracellular pH of a suspension of glucose-deprived RBCs decreased over time, with the pH changing more rapidly in the extracellular medium (Figure 4.7). The rate of change in pH was slightly faster in the presence of NADH in both compartments; hence, it was not possible from the pH data alone to determine the site of lactate formation.

^{31}P NMR spectra also indicated that the rate of decrease in the concentration of 2,3BPG in the presence of NADH was similar to that observed in control glucose-deprived RBCs (Figure 4.6). Hence the formation of lactate in the presence of extracellular NADH was not due to an increased formation of pyruvate from 2,3BPG, but rather from an increase in the conversion of pyruvate to lactate at the LDH reaction.

The transport of anions via band 3 across the plasma membrane was not essential for the oxidation of extracellular NADH by glucose-deprived RBCs. Band 3 is the most abundant transport protein in the RBC membrane and catalyses the one-for-one exchange of anions across the plasma membrane (Falke and Chan, 1986) and H^+-anion exchange at a much slower rate (Jennings, 1976). It is partially inhibited by DIDS which covalently binds to a lysine residue near the transport site, reducing the affinity of the transporter for chloride ions (Zou, *et al.*, 2000). DIDS has also been reported to increase the rate of lysis of RBCs (Falke and Chan, 1986). Incubation of glucose-deprived RBCs with 0.1 mM DIDS prior to exposure to NADH had no effect on the observed rates of lactate and pyruvate formation compared to RBCs not exposed to DIDS (Figure 4.4). Surprisingly, DIDS also had no effect on the rate of equilibration of MeP or P_i across the plasma membrane; both substances enter the cell via band 3 (Stewart, *et al.*, 1986). The result with P_i may have been due to the relatively high concentration (25 mM) of the phosphate buffer used. DIDS also had no effect on the rate of 2,3BPG utilisation in the absence of NADH, however the rate was decreased in the presence of NADH.

αCHC has been shown to competitively inhibit the transport of both pyruvate and lactate into RBCs (K_i ~50–60 μM) via inhibition of the monocarboxylate transporter

(Halestrap and Denton, 1974; Halestrap, 1976). Thus, αCHC was expected to affect the NADH-induced changes in RBC metabolism. Incubation of glucose-starved RBCs with αCHC significantly changed the rates of lactate and pyruvate production compared to control cells not exposed to αCHC (Figure 4.4). Lactate production was stimulated, though not to the same extent as with NADH, and the rate of lactate production by RBCs incubated with αCHC and exposed to NADH was slightly attenuated compared to the rate with NADH alone (Figure 4.4). Incubation of RBCs with αCHC also decreased the rate of 2,3BPG utilisation in both the presence and absence of NADH (Figure 4.6). The rate of NADH oxidation by these RBCs was also observed to be lower. Thus it appears that αCHC, by blocking the equilibration of lactate and pyruvate across the membrane, results in a change in the RBC metabolism. αCHC is transported into RBCs via the monocarboxylate transporter (Halestrap and Denton, 1975), and has been shown to inhibit the entry of pyruvate into mitochondria of other cell lines. αCHC at concentrations up to 2 mM has been shown to have no effect on LDH activity in epididymal fat-pads, but at concentrations significantly higher than those required for pyruvate transport inhibition (1 mM); pyruvate carboxylase is inhibited (Halestrap and Denton, 1975). The high concentrations of αCHC used in these experiments (50 mM) may have led to the inhibition of enzymes of the lower part of the glycolytic pathway, and in particular LDH.

The results obtained with inhibitors did not confirm the hypothesis that extracellular NADH transferred reducing equivalents to intracellular NAD^+. The αCHC results suggest that the movement of monocarboxylates such as pyruvate and lactate is necessary, at least in part, for changes in RBC metabolism during starvation to be induced by NADH. In order to clarify the location of lactate formation, RBCs were starved for 2 h ensuring a build up of pyruvate then exposed to NADD. ^1H spin-echo NMR experiments showed that the lactate that was formed was deuterated at the C-2 position (Figure 4.10). This result suggests that the lactate was formed in the extracellular medium as the RBC membrane is impermeable to NADD (see §5.3.3). After 2 h of glucose starvation the LDH activity in the supernatant was ~3% of that observed in whole cells at the same time (Figure 4.14). Thus, [2-^2H]lactate can be formed in the extracellular medium from reaction of pyruvate and NADD catalysed

by extracellular LDH. Equilibration of [2-^{2}H]lactate across the membrane will lead to deuteration of NAD^+ inside the cell and hence increased intracellular [2-^{2}H]lactate. Although the majority of lactate formed in the presence of NADD was deuterated, it is not clear whether there were other mechanisms of extracellular NADH oxidation other than by extracellular LDH. The addition of L-[U-^{2}H]lactate to glucose-supplied RBCs has previously been shown to result in the diminution of the inverted resonance from endogenous L-lactate in ^{1}H spin-echo NMR spectra; this was brought about through equilibration of the reactants via LDH activity (Berthon and Kuchel, 1995).

The involvement of LDH in the NADH-induced changes in metabolism of starved RBCs was investigated further by adding LDH inhibitors, oxalate and oxamate, to the incubation medium. Oxamate is a competitive inhibitor with respect to pyruvate and non-competitive with respect to lactate (Nisselbaum, *et al.*, 1964), while oxalate is competitive with respect to lactate and non-competitive with respect to pyruvate (Nisselbaum, *et al.*, 1964). Oxalate also binds to both the enzyme-NADH and enzyme NAD^+ complexes, with preferential binding to the latter (Mazo, *et al.*, 1990). Isolated guinea pig skeletal muscle LDH activity is decreased by 99% with 6 mM oxamate and 92% by 6 mM oxalate (Mazo, *et al.*, 1990). Oxalate penetrates the RBC membrane at a similar rate to lactate and pyruvate at 37 °C (Halestrap, 1976; Brindle, *et al.*, 1979; Hubbard, *et al.*, 1980; Simpson, *et al.*, 1982), and has an apparent inhibition constant for LDH of 0.9 mM (Simpson, *et al.*, 1982). Both oxalate and oxamate inhibited the effect of NADH and pyruvate on the rate of lactate formation (Figure 4.13, Table 4.1). The rate of pyruvate utilisation decreased in tandem with that of lactate production, maintaining the same change in the lactate-to-pyruvate ratio as the concentrations of the inhibitors were increased. Thus oxalate and oxamate inhibited both intra- and extracellular LDH activity. This was confirmed by the increased inhibition observed after pre-incubating RBCs with either oxalate or oxamate prior to addition of NADH and pyruvate (Table 4.1). Pre-incubation ensured that intracellular LDH activity was inhibited prior to the experiment. Washing these cells immediately prior to the addition of NADH and pyruvate, removed the majority of the extracellular LDH activity. The rate of lactate

production was decreased further by the addition of oxalate and oxamate to cells already exposed to these compounds.

Thus the effects of NADH on the end products of RBC metabolism appear to be due to the presence of LDH in the extracellular medium. However, because of the incomplete inhibition by oxalate and oxamate and the variable nature of the effect with 100 μM capsaicin (inhibition in absence and stimulation in presence of pyruvate) it was difficult to determine the fine details of the kinetics of these reactions. The rates of lactate formation and NADH oxidation by freshly washed RBCs exposed to NADH and pyruvate were surprisingly high considering that less than 0.5% of the cells would have lysed in the first 30 min of the incubation. Hence I investigated the involvement of LDH in the effects of NADH and the location of the NADH oxidation site in greater detail, and present the results in the following Chapter.